

Cu and Zn in the early Galaxy

G. Bihain¹, G. Israelian¹, R. Rebolo^{1,2}, P. Bonifacio³, and P. Molaro³

¹ Instituto de Astrofísica de Canarias, c/ Vía Láctea, s/n, 38205 La Laguna, Tenerife, Spain
e-mail: [gbihain;gil;rr1]@ll.iac.es

² Consejo Superior de Investigaciones Científicas, Spain

³ Istituto Nazionale di Astrofisica, Osservatorio Astronomico di Trieste, via G. B. Tiepolo 11, 34131 Trieste, Italy
e-mail: [molaro;bonifacio]@ts.astro.it

Received 19 December 2003 / Accepted 27 April 2004

Abstract. We present Cu and Zn abundances for 38 FGK stars, mostly dwarfs, spanning a metallicity range between solar and $[\text{Fe}/\text{H}] = -3$. The abundances were obtained using Kurucz's local thermal equilibrium (LTE) model atmospheres and the near-UV lines of Cu I 3273.95 Å and Zn I 3302.58 Å observed at high spectral resolution. The trend of $[\text{Cu}/\text{Fe}]$ versus $[\text{Fe}/\text{H}]$ is almost solar for $[\text{Fe}/\text{H}] > -1$ and then decreases to a plateau $\langle [\text{Cu}/\text{Fe}] \rangle = -0.98$ at $[\text{Fe}/\text{H}] < -2.5$, whereas the $[\text{Zn}/\text{Fe}]$ trend is essentially solar for $[\text{Fe}/\text{H}] > -2$ and then slightly increases at lower metallicities to an average value of $\langle [\text{Zn}/\text{Fe}] \rangle = +0.18$. We compare our results with previous work on these elements, and briefly discuss them in terms of nucleosynthesis processes. Predictions of halo chemical evolution fairly reproduce the trends, especially the $[\text{Cu}/\text{Fe}]$ plateau at very low metallicities, but to a lesser extent the higher $[\text{Zn}/\text{Fe}]$ ratios at low metallicities, indicating possibly missing yields.

Key words. stars: Population II – stars: abundances – Galaxy: evolution

1. Introduction

Massive, low- and intermediate-mass stars, type II and type Ia supernovae are likely contributors to the Galactic chemical evolution of Cu and Zn. However, the nucleosynthesis mechanisms and the relative contributions of the nucleosynthesis sites for these near-iron-peak nuclei are still uncertain. The abundances of Cu in metal-poor stars with $[\text{Fe}/\text{H}] > -1.7$ have been comprehensively reviewed by Peterson (1981), with no significant deviation from the solar ratio $[\text{Cu}/\text{Fe}] = 0$. Further studies by Luck & Bond (1985), Sneden & Crocker (1988) and Sneden et al. (1991) show that, while the $[\text{Zn}/\text{Fe}]$ ratio remains essentially solar, there is in fact a clear decrease in $[\text{Cu}/\text{Fe}]$ at lower metallicities, consistent with previous results for the metal-poor globular clusters M 13 and M 92 by Cohen (1978, 1979, 1980). This departure from the solar ratio is as noticeable as for the iron peak elements Cr, Mn and Co; $[\text{Co}/\text{Fe}]$, however, is increasing at lower metallicities (e.g. Cayrel et al. 2003). More recent studies (Mishenina et al. 2002; Simmerer et al. 2003) show that the trend of Cu is non-linear in metal-poor stars and globular clusters, which presumably results from the superposition of Fe-independent (“primary”) and Fe-dependent (“secondary”) nucleosynthesis mechanisms. While there is a general consensus on the early contribution by short-lived massive stars, there are many uncertainties concerning how these stars produce Cu and Zn, and how their yields lead to the observed low-metallicity tails of the ratio distributions.

The above-mentioned studies are performed mostly with optical lines¹ (Cu I at 5105.54 Å, 5218.20 Å and 5782.12 Å; Zn I at 4722.16 Å, 4810.53 Å and 6362.35 Å). These lines become very weak in the spectra of very metal-poor stars. Therefore we decided to explore the use of the UV lines Cu I 3273.95 Å and Zn I 3302.58 Å, which are quite intense in the solar spectrum and, in the case of the Cu line, potentially detectable at very low metallicities ($[\text{Fe}/\text{H}] < -3$). In the following sections, we will discuss the observations, their analysis, and how these lines are indeed useful for investigating the chemical evolution of copper and zinc at low metallicities.

2. Observations

The studied sample contains 38 FGK metal-poor stars, principally dwarfs. Most of the high-resolution spectra were obtained at the 4.2 m WHT/UES (La Palma) during 1992–1993. Spectra of the stars HD 3795, LHS 540, HD 211998, HD 166913, HD 218502 and HD 128279 were obtained at the 3.6 m/CASPEC (La Silla) during 1993; and of the stars HD 22879 and HD 132475 at the 3.9 m AAT/UCLES (Siding Spring) during 1990–1991. The spectra of the very metal-poor stars LP 815-43, G275-4 and G64-12 were obtained at the 8.2 m VLT Kueyen/UVES (Paranal) during 1999–2000 (see details in Israelian et al. 2001). Finally, the spectra of the very

¹ In a study of stellar abundances in the thick disc of the Galaxy (Prochaska et al. 2000), the IR line Cu I 8092 Å is also used.

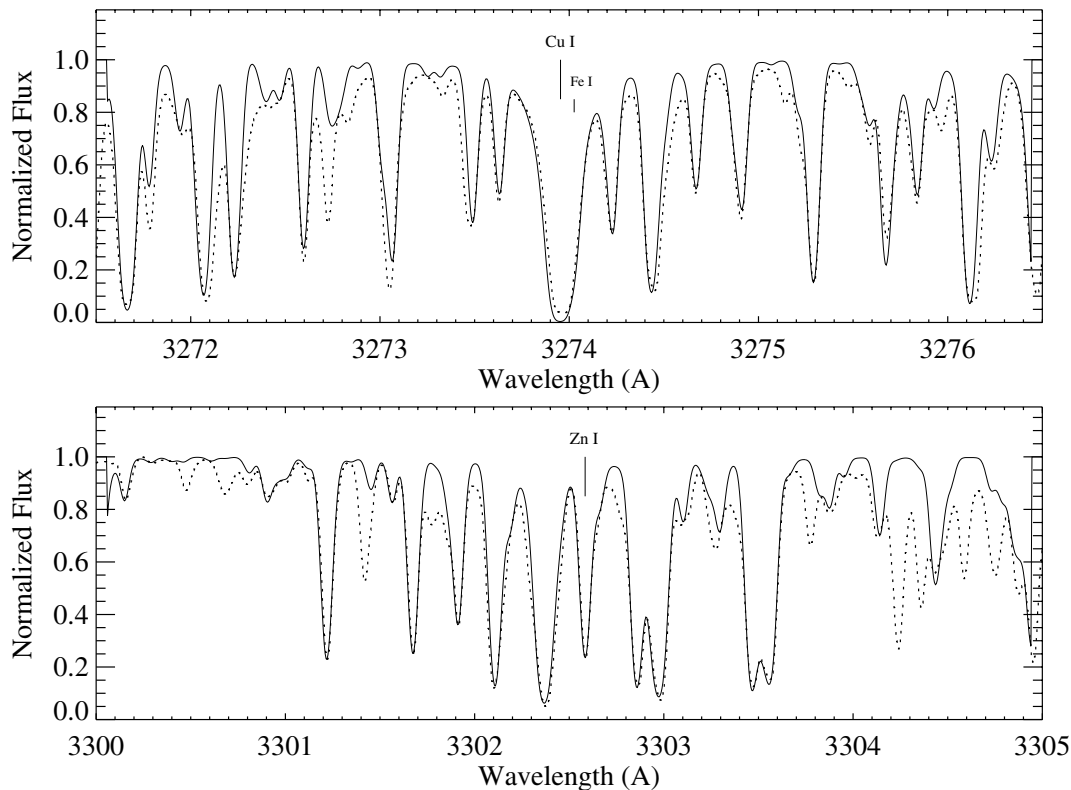


Fig. 2. Expanded plots of the solar spectral regions (*dotted lines*) fitted with the synthetic spectrum (*solid lines*).

and those of the Zn I line at 3302.58 \AA ($\log gf = -0.057$, $\chi = 4.030$) were taken from VALD-2 (Kupka et al. 1999). The wavelengths and the relative strengths of the hyperfine components of the copper isotopes ^{63}Cu and ^{65}Cu were obtained from Kurucz (2003, private communication), and the solar isotopic ratio was adopted from Anders & Grevesse (1989) for all the stars. The oscillator strengths of the lines were calibrated with the solar spectrum, using a model atmosphere with overshooting from Kurucz (1992, private communication) for the parameters $T_{\text{eff},\odot} = 5777 \text{ K}$, $\log g_{\odot} = 4.438$, $V_{\text{L},\odot} = 1,0 \text{ km s}^{-1}$ and the Unsöld damping approximation without enhancement. The calibration provided $\log gf = -0.167$ for the Zn I line (see Fig. 2). In the case of the Cu I lines $\log gf$ was not modified, because its modification strongly affected the suitable fit to the wings (as obtained from the *cog* driver of MOOG, the lines were in the linear damping part of the curve of growth) and did not improve the fit to the cores. In fact, the cores of such lines are usually formed close to the chromospheric temperature minimum, which exceeds that of the upper photosphere. Since no chromosphere is included in our model, these cores could not be reproduced as in the observed spectrum.

Stellar parameters for the model atmospheres were obtained as follows. The effective temperatures (T_{eff}) were estimated using the Alonso et al. (1996, 1999b) calibrations versus $V - K$ colours for dwarfs and giants, respectively. The V magnitudes were taken from the Hipparcos Catalog (Perryman et al. 1997), Alonso et al. (1994) or else from the SIMBAD database. The K magnitudes were taken from Alonso et al. (1994, 1998), or else from Carney & Aaronson (1979; HD 170153, HD 165908, HD 225239 and HD 157214) and

Laird et al. (1988; G170-47). For HD 166913, a K_s magnitude was taken from the 2MASS Catalogue, and then converted to K using a relation determined from a comparison of the magnitudes in these bands for similar stars in the sample. Since no accurate K or K_s values were available for the stars HD 211998 and HD 3795, the $T_{\text{eff}}-(B - V)$ calibrations from Alonso et al. (1996, 1999b) were used, with $(B - V)$ from the Hipparcos Catalogue or the SIMBAD database. LTE metallicities were adopted from the literature, mainly from Fulbright (2000), Mishenina et al. (2002) and Thévenin (1998). The differences in the values provided by these three sources were typically not greater than 0.12 dex for the stars in common, therefore justifying the use of an average metallicity (see Table 1). Finally, the initial surface gravities were taken from the same references, with the exception of Thévenin & Idiart (1999) which was used instead of Thévenin (1998), because a higher priority was given to their NLTE $\log g$ values (see comments below). Stars with surface gravities $\log g > 3.5$ were classified as dwarfs, while stars with $\log g < 2.5$ were classified as giants, so that the corresponding T_{eff} colour calibration was used for each group. When stars had an intermediate $\log g$ value, T_{eff} was adopted as the average of the temperatures obtained with the calibrations for dwarfs and for giants, respectively.

We found a very good agreement between our T_{eff} values and the spectroscopic T_{eff} values from Mishenina & Kovtyukh (2001) for the 23 stars in common, $\langle T_{\text{eff}} - T_{\text{eff,MK}} \rangle = +26 \text{ K}$, with a standard deviation $\sigma = 75 \text{ K}$ (see Fig. 3). A comparison with the spectroscopic T_{eff} values from Fulbright (2000), however, showed a systematic difference of $\langle T_{\text{eff}} - T_{\text{eff,F}} \rangle = +99 \text{ K}$ with $\sigma = 82 \text{ K}$ (25 stars). Since the 21 stars for this

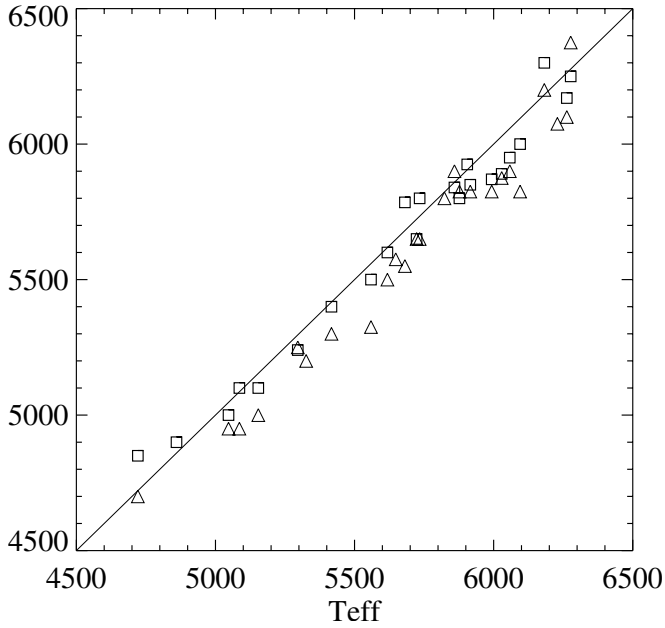


Fig. 3. Comparison of the T_{eff} obtained in this study with spectroscopic T_{eff} from Fulbright (*triangles*) and Mishenina & Kovtyukh (*squares*).

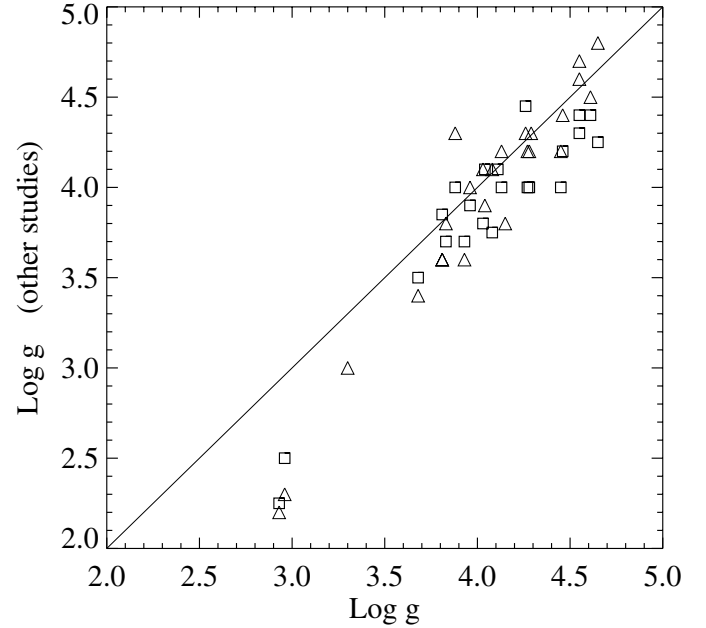


Fig. 4. Comparison of the $\log g$ obtained in this study with spectroscopic $\log g$ from Fulbright (*triangles*) and Mishenina & Kovtyukh (*squares*).

latter comparison were also included in the comparison with Mishenina & Kovtyukh's sample, this difference should be attributed to the different methods used. Fulbright determines an excitation temperature for the dwarfs (by requiring the same iron abundance for Fe I lines with high and low excitation potential), whereas Mishenina & Kovtyukh determine a temperature from the fits to the wings of the H_{α} lines. Comparing with Thévenin's (1998) T_{eff} values, we found $\langle T_{\text{eff}} - T_{\text{eff,T}} \rangle = +79$ K with $\sigma = 97$ K (23 stars). These are selected from the catalogue of Cayrel de Strobel et al. (1992), and redetermined from colours in the rare case that they are initially determined from Fe I lines (Thévenin 2003, private communication). Comparing for the remaining stars, we found similar values to those in the references used for the metallicities, with a difference of less than 80 K, apart for the star HD 128279, for which we obtained 5130 K, and Gratton et al. (2000) obtain 5394 K. This latter value is derived from dereddened $(B - V)_0$ and $(b - v)_0$ colours using colour- T_{eff} transformations (Kurucz 1995), and is higher, as for nearly all the stars in common with the present sample.

The surface gravities ($\log g$) were estimated using Hipparcos parallaxes (Perryman et al. 1997) through the relation proposed by Nissen et al. (1997), $[g] = [M] + 4 [T_{\text{eff}}] + 0.4 (M_{\text{bol}} - M_{\text{bol},\odot})$, where $[x] = \log x/x_{\odot}$. The solar bolometric magnitude $M_{\text{bol},\odot} = 4.75$ mag was taken from Allen (1976), and the bolometric magnitudes of the stars were determined using interpolated bolometric corrections from the grids given by Alonso et al. (1999a): $M_{\text{bol}} = K + \text{BC}(K) + 5 \log \pi + 5$, where π is the trigonometric parallax. For the two stars without accurate K and K_s magnitudes $\text{BC}(V)$ was interpolated from the grids of Alonso et al. (1995, 1999b). The relative standard error in parallax, $\sigma(\pi)/\pi$, was typically of order 0.10 and smaller than 0.30. The stellar masses (M) were derived from their

position in the $(\log T_{\text{eff}}, \log L/L_{\odot})$ plane, using the isochrones from Bergbusch & Vandenberg (2001). Most of the stars were found to be in the main sequence and the subgiant domain, while the remainder were in the red giant branch. The average stellar mass for the sample was $0.78 M_{\odot}$. The error in $\log g$ arose mainly from the parallax uncertainty: an error of $\sigma(\pi)/\pi = 0.10$ implied (via the bolometric magnitude) $\Delta \log g = 0.10$ dex, while typical errors in the mass $\sigma(M) = 0.045 M_{\odot}$ and in the effective temperature $\sigma(T_{\text{eff}}) = 75$ K implied errors of only $\Delta \log g = 0.025$ dex.

The surface gravities of the dwarf stars agreed in general with the LTE spectroscopic values from Fulbright (2000) and Mishenina & Kovtyukh (2001), see Fig. 4. However, those of the very metal-poor subgiants HD 87140 and G170-47 were different, with $\Delta \log g > +0.40$ dex. This discrepancy between trigonometric and LTE spectroscopic surface gravities in late-type stars is discussed by Nissen et al. (1997) and Allende Prieto et al. (1999). Moreover, trigonometric surface gravities agree better with NLTE spectroscopic determinations (Thévenin & Idiart 1999). Since no NLTE value is published for HD 87140, we could only compare with a trigonometric value, for instance that given by Gratton et al. (2000) and we found a difference of 0.05 dex. For G170-47, we could compare with the NLTE "best choice" determination from Israelian et al. (2001) and found a difference of 0.07 dex. As for the remaining stars, we found $\log g$ values very similar to those in the references we used for metallicities, with differences of less than 0.17 dex.

For the three very metal-poor dwarfs G64-12, G275-4 and LP815-43 observed with VLT/UVES, the atmospheric parameters were taken from Israelian et al. (2001). For the two very metal-poor giants BD -18°5550 and HD 2796, the

Table 1. Stellar atmospheric parameters and Cu and Zn abundances. Some parameters are from 1) Castro et al. (1999); 2) Chen et al. (2000); 3) Fulbright (2000); 4) Spite & Spite (1982); 5) Gratton et al. (2000); 6) Mishenina et al. (2002); 7) Thévenin (1998); 8) Israelian et al. (2001); 9) Israelian & Rebolo (2001). Solar Cu and Zn abundances are from Anders & Grevesse (1989).

Star	T_{eff} K	$\log g$	V_t km s $^{-1}$	[Fe/H]	Ref.	[Cu/H]	σ	[Zn/H]	σ
G64-12	6318 (150) ⁸	4.20 (.3) ⁸	1.0	-3.05 ⁸	c	-4.00	0.18	<-2.35	-
BD -18°5550	4668 (63) ⁹	1.5 (.3) ⁹	1.5	-3.01 ⁶	b	-3.94	0.20	-2.81	0.17
G275-4	6212 (150) ⁸	4.13 (.3) ⁸	1.0	-2.99 ⁸	c	-3.85	0.18	<-2.34	-
BD +3°740	6229 (67)	4.15 (.27)	1.0	-2.82 ^{3,7}	b	<-3.77	-	<-2.02	-
LP 815-43	6265 (125) ⁸	4.54 (.3) ⁸	1.0	-2.74 ⁸	c	-3.79	0.15	<-2.29	-
G170-47	5154 (58)	2.93 (.28)	1.25	-2.66 ^{3,6}	b	-3.76	0.19	<-2.21	-
HD 140283	5723 (67)	3.68 (.06)	1.0	-2.47 ^{3,6,7}	b	-3.42	0.14	-2.27	0.14
BD +26°3578	6263 (76)	3.93 (.21)	1.0	-2.36 ^{3,6,7}	b	-3.01	0.14	<-1.96	-
HD 2796	4860 (46)	1.80 (.2) ⁹	1.5	-2.18 ^{6,7}	b	-	-	-2.03	0.17
BD +37°1458	5326 (54)	3.30 (.23)	1.25	-2.17 ³	b	-2.87	0.14	-1.82	0.12
HD 128279	5130 (66)	2.85 (.22)	1.25	-2.11 ⁵	a	-3.11	0.20	-2.31	0.17
HD 84937	6277 (75)	4.03 (.09)	1.0	-2.06 ^{3,6,7}	b	-2.96	0.14	<-1.96	-
HD 19445	6095 (69)	4.45 (.05)	1.0	-2.04 ^{3,6,7}	b	-2.69	0.14	-1.69	0.12
HD 87140	5086 (43)	2.96 (.31)	1.25	-1.83 ^{3,6}	b	-2.28	0.21	<-1.13	-
HD 25329	4721 (65)	4.65 (.06)	1.0	-1.78 ^{3,6,7}	b	-2.23	0.20	-	-
HD 218502	6182 (77)	4.08 (.08)	1.0	-1.76 ^{3,6,7}	a	-2.51	0.17	-1.61	0.12
HD 64090	5417 (65)	4.55 (.06)	1.0	-1.74 ^{3,6,7}	b	-2.19	0.20	-1.64	0.16
HD 166913	6181 (74)	4.18 (.07)	1.0	-1.68 ⁷	a, d	-1.88	0.41	-1.23	0.25
HD 132475	5648 (69)	3.81 (.10)	1.0	-1.60 ^{3,7}	d	-2.10	0.25	-1.10	0.18
HD 188510	5559 (65)	4.55 (.06)	1.0	-1.57 ^{3,6}	b	-1.88	0.24	-1.52	0.20
BD +23°3912	5734 (67)	3.83 (.13)	1.0	-1.50 ^{3,6,7}	b	-1.90	0.25	-	-
HD 94028	6058 (72)	4.27 (.06)	1.0	-1.49 ^{3,6,7}	b	-1.79	0.29	-1.39	0.17
HD 211998	5282 (180)	3.28 (.28)	1.25	-1.48 ⁷	a, d	-2.10	0.34	-1.43	0.14
LHS 540	5993 (71)	3.88 (.20)	1.0	-1.48 ^{3,6}	a	-1.63	0.26	-1.33	0.12
HD 103095	5047 (68)	4.61 (.05)	1.0	-1.43 ^{3,6,7}	b	-1.83	0.16	-1.38	0.11
HD 194598	6029 (77)	4.28 (.07)	1.0	-1.20 ^{3,6,7}	b	-1.45	0.32	-	-
HD 189558	5681 (70)	3.81 (.08)	1.0	-1.12 ^{3,6,7}	b	-1.42	0.21	-1.02	0.16
HD 201891	5916 (77)	4.26 (.05)	1.0	-1.05 ^{3,6,7}	b	-0.95	0.26	-0.85	0.12
HD 201889	5618 (67)	4.04 (.08)	1.0	-0.95 ^{3,6,7}	b	-1.00	0.21	-0.80	0.16
HD 22879	5823 (70)	4.29 (.04)	1.0	-0.91 ³	d	-1.16	0.25	-0.76	0.18
HD 76932	5859 (72)	4.13 (.04)	1.0	-0.90 ^{3,6,7}	b	-1.02	0.21	-0.74	0.16
HD 6582	5296 (67)	4.46 (.05)	1.0	-0.86 ^{3,6,7}	b	-0.96	0.17	-0.91	0.11
HD 134169	5877 (72)	3.96 (.07)	1.0	-0.81 ^{3,6,7}	b	-0.66	0.21	-0.81	0.16
HD 3795	5226 (185)	3.78 (.07)	1.0	-0.70 ¹	a	-0.85	0.34	-0.75	0.12
HD 165908	5905 (42)	4.11 (.03)	1.0	-0.67 ⁶	b	-0.67	0.24	-0.67	0.12
HD 170153	5954 (42)	4.13 (.03)	1.0	-0.65 ²	b	-0.70	0.24	-0.60	0.12
HD 225239	5528 (44)	3.74 (.15)	1.0	-0.5 ⁴	b	-0.56	0.18	-0.54	0.16
HD 157214	5715 (43)	4.21 (.03)	1.0	-0.35 ⁷	b	-0.40	0.16	-0.35	0.16

a. CASPEC- 3.6 m Telescope; b. UES- WHT; c. UVES- VLT; d. UCLES- AAT.

spectroscopic $\log g$ and T_{eff} were taken from Israelian & Rebolo (2001). Finally, the microturbulence was fixed at $V_t = 1.0 \text{ km s}^{-1}$ for the dwarfs and 1.5 km s^{-1} for the giants.

3.1. Cu and Zn abundances

The abundances of Cu and Zn are listed in Table 1. The wings of the intense Cu I lines were fitted with the synthetic spectrum by differential analysis with respect to the Sun. Because these lines were in the damping or saturation parts of the curve of growth for stars with solar temperature and

metallicities $-2 < [\text{Fe}/\text{H}] < 0$, the effects of changing the abundances were carefully checked. In general an uncertainty of 0.1 dex was adopted for the derived abundances. For metallicities lower than -2 the lines were unsaturated, and the adjustments could be achieved more precisely.

The uncertainties in T_{eff} and $\log g$ led to average errors of respectively 0.11 and 0.02 dex in the Cu abundance, and 0.035 and 0.02 dex in the Zn abundance, while the V_t uncertainty led to an average error of 0.07 in the Cu abundance and 0.05 dex in the Zn abundance. The main contribution to the error came

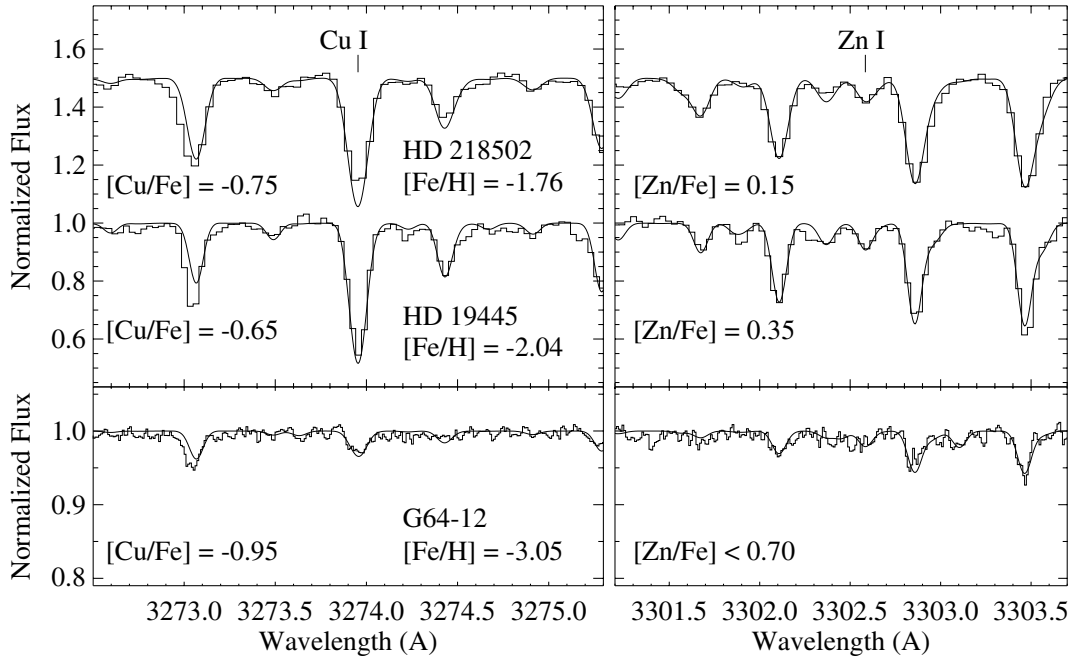


Fig. 5. Synthetic spectral fits to the copper and zinc lines in the spectra of several metal-poor stars of our sample.

Table 2. Sensitivities of the copper and zinc abundances to variations in the atmospheric parameters of the stars HD 94028 ($T_{\text{eff}} = 6058$ K, $\log g = 4.28$, $V_t = 1.0$ km s $^{-1}$), HD 140283 ($T_{\text{eff}} = 5723$ K, $\log g = 3.68$, $V_t = 1.0$ km s $^{-1}$) and G170-47 ($T_{\text{eff}} = 5154$ K, $\log g = 2.93$, $V_t = 1.25$ km s $^{-1}$), and to the overshooting.

	HD 94028				HD 140283				G170-47			
	T_{eff}	$\log g$	V_t	Os	T_{eff}	$\log g$	V_t	Os	T_{eff}	$\log g$	V_t	Os
	+100	+0.30	-0.3	off	+100	+0.30	-0.3	off	+100	+0.30	-0.3	off
[Cu/H]	+0.15	-0.06	+0.13	-0.15	+0.12	0.00	+0.02	-0.13	+0.13	0.00	+0.04	-0.15
[Zn/H]	+0.06	+0.03	+0.01	-0.10	+0.06	+0.04	0.00	-0.10	+0.04	+0.04	0.00	-0.09

from the uncertainty in the localization of the continuum, especially in the spectra of the more metal-rich stars and in the noisy spectra; this uncertainty implied an error of 0.1–0.2 dex in the abundances. Additionally the noise in the copper and zinc lines led to an error of 0.05–0.1 dex. In the case of the Cu I $\lambda 3273.95$ Å line, an extra error of 0.01–0.04 dex was taken into account for the uncertainty in the contribution of the weak Fe I $\lambda 3273.95$ Å line.

A few spectra also permitted the analysis of the other Cu I line at 3247.54 Å. In the case of the very metal-poor dwarfs G64-12, G275-4, LP 815-43, an agreement to within 0.15 dex was found between the Cu abundances given by the two lines. Those in the spectrum of the giant BD $-18^{\circ}5550$, however, provided a difference of 0.25 dex, suggesting that the differential analysis with respect to the Sun was less reliable for this star (note that for the other giant, HD 2796, the difference was still greater, reason why its Cu abundance was not listed in Table 1). As for the zinc line, the spectra of only six stars out of the thirteen with $[\text{Fe}/\text{H}] < -2$ permitted a clear detection. The spectra of the remaining stars presented a very weak feature at 3302.58 Å, from which no reliable abundance could be derived; thus upper limits to the abundances were established. Figure 5 shows the fits for three metal-poor stars.

Since Kurucz’s models atmospheres without overshooting give a better reproduction of colour indices, Balmer profiles and Procyon data than Kurucz’s models with overshooting (Castelli et al. 1997), we checked the changes produced on the abundances using the former models. For the stars HD 94028, HD 140283 and G147-70 (Table 2), these models implied Cu and Zn abundances systematically lower by about 0.15 and 0.10 dex, respectively, differences small enough to preserve the main properties of our results discussed in Sect. 4.

As found by Cayrel et al. (2003), the abundances derived from the spectra of metal-poor stars may be overestimated if the continuum scattering is approximated as an additional opacity source in the spectral synthesis code. The overestimation is especially high for $\lambda < 400$ nm, where continuum scattering becomes important relative to continuous absorption. Since the spectral synthesis code MOOG approximates scattering by absorption, we evaluated the influence on the abundances by using another LTE spectral synthesis code, TurboSpectrum (Alvarez & Plez 1998), which takes proper account of the continuum scattering. For the only two giants, HD 2796 and BD $-18^{\circ}5550$, the Cu abundances derived using TurboSpectrum were lower by more than 0.2 dex than those derived using MOOG, while the Zn abundances were the same.

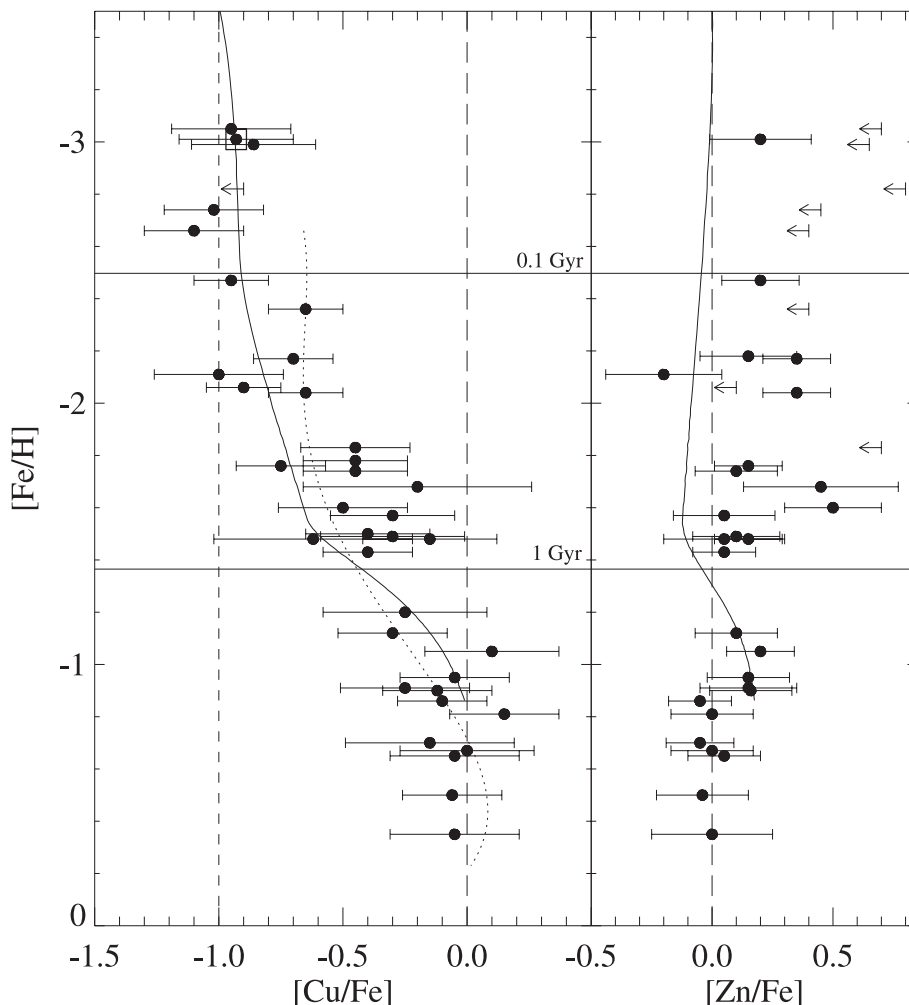


Fig. 6. $[\text{Cu}/\text{Fe}]$ and $[\text{Zn}/\text{Fe}]$ ratios vs. $[\text{Fe}/\text{H}]$. The upper limits of Zn abundances are represented by the *arrows*, the Cu abundance in the giant BD $-18^{\circ}5550$ by the *square* and the fit to the Cu data obtained by Mishenina et al. by the *dotted line*. The *solid lines* represent the predictions of the Prantzos model and the *horizontal lines* represent the elapsed time since the beginning of the halo formation.

As for the dwarfs G275-4 and G64-12, the abundances for both elements were higher by less than $+0.1$ dex. We therefore concluded that, for the dwarfs, the Cu and Zn abundances obtained from the UV lines were not significantly affected by this source of errors, while for the giants only the Zn abundances were. We thus removed the contribution of the giants from our conclusion on the Cu trend.

We compared our Cu and Zn abundances with those of Mishenina et al. (2002) obtained from optical lines, and found a good agreement: $\Delta[\text{Cu}/\text{H}] = \langle [\text{Cu}/\text{H}] - [\text{Cu}/\text{H}]_M \rangle = -0.04$ dex, with a standard deviation $\sigma = 0.15$ dex (16 stars; no giant data to compare), and $\Delta[\text{Zn}/\text{H}] = 0.03$ dex, with $\sigma = 0.13$ dex (16 stars), respectively. Converting our values with our abundance sensitivities to their adopted stellar atmospheric parameters provided a similar agreement: $\Delta[\text{Cu}/\text{H}] = -0.09$ dex, with $\sigma = 0.14$ dex, and $\Delta[\text{Zn}/\text{H}] = -0.02$ dex, with $\sigma = 0.13$ dex, respectively. The slight abundance decrease was due principally to their lower effective temperatures and microturbulence. The dwarf HD 19445 (see Fig. 5) was the most metal-poor star for Cu abundance comparison with Mishenina et al. (2002), with $[\text{Fe}/\text{H}] = -2.04$. We found $[\text{Cu}/\text{H}] = -2.69$, a value 0.37 dex

lower than that of Mishenina et al. (2002), and lower by ~ 0.1 dex than the upper limit estimate of Sneden et al. (1991) (for their adopted atmospheric parameters). We also compared our results with the abundances obtained from optical lines by Sneden et al. (1991), and we found a rough agreement for Cu, $\Delta[\text{Cu}/\text{H}] = 0.13$ dex, with $\sigma = 0.36$ dex (5 stars only³; no giant data to compare), and for Zn, $\Delta[\text{Zn}/\text{H}] = 0.13$ dex, with $\sigma = 0.13$ dex (8 stars), respectively. Converting our values with our abundance sensitivities to their adopted stellar atmospheric parameters also revealed a rough agreement for Cu, $\Delta[\text{Cu}/\text{H}] = 0.17$ dex, with $\sigma = 0.24$ dex, and a good agreement for Zn, $\Delta[\text{Zn}/\text{H}] = 0.04$ dex, with $\sigma = 0.14$ dex, respectively.

4. Trends of $[\text{Cu}/\text{Fe}]$ and $[\text{Zn}/\text{Fe}]$

4.1. Results

Our derived $[\text{Cu}/\text{Fe}]$ and $[\text{Zn}/\text{Fe}]$ ratios are shown in Fig. 6. The $[\text{Cu}/\text{Fe}]$ ratio is almost solar down to $[\text{Fe}/\text{H}] \sim -1$ and

³ The stars were less metal-poor than HD 19445 and common to the sample of Mishenina et al. (2002).

then decreases, until it reaches a plateau $\langle[\text{Cu}/\text{Fe}]\rangle = -0.98$ at $[\text{Fe}/\text{H}] < -2.5$ (the ratio is averaged over the five stars that are not giants). This slanted s-shape trend in dwarfs is similar to that outlined by Mishenina et al. (2002) (see Fig. 6). However, the $[\text{Cu}/\text{Fe}]$ plateau is ~ 0.3 dex lower than the plateau obtained in the range $-2.7 < [\text{Fe}/\text{H}] < -1.7$ in their halo giants and in the globular clusters studied by Simmerer et al. (2003). It could be noticed that underabundances near $[\text{Cu}/\text{Fe}] = -1$ are also found in Mishenina et al. (2002) (the two dwarfs BD +41°3931 and HD 140283⁴, Fig. 9, with $[\text{Cu}/\text{Fe}] = -0.97$ and ~ -0.95 , respectively) and in Sneden et al. (1991) (the giants HD 2665 and HD 122563, Fig. 7, with $[\text{Cu}/\text{Fe}] = -0.87$ and -0.93). In addition, Sneden et al. (1991) provide an upper limit $[\text{Cu}/\text{H}] < -3.93$ for the giant BD -18°5550, and we find $[\text{Cu}/\text{H}] = -3.94$ ($[\text{Cu}/\text{Fe}] = -0.93$), a value that would be even lower if we were to take into account a better treatment of the UV spectral synthesis (see Sect. 3.1).

Considering zinc, the $[\text{Zn}/\text{Fe}]$ ratio is essentially solar down to $[\text{Fe}/\text{H}] \sim -2.0$, with a possible excess of $\langle[\text{Zn}/\text{Fe}]\rangle = +0.18$ at lower metallicities. It is interesting to compare our results with existing high quality surveys which include observations of Zn: those of Mishenina et al. (2002) and Gratton et al. (2003) in a metallicity range comparable to that of this study, and that of Cayrel et al. (2003), which is complementary and covers considerably lower metallicities. The comparison of our data with those of these three studies is shown in Fig. 7. The ensemble of all the data gives a clear picture of the evolution of the Zn/Fe ratio with metallicity. A solar ratio of Zn/Fe is supported by the data of both Mishenina et al. (2002) and Gratton et al. (2003) down to a metallicity of about $[\text{Fe}/\text{H}] \sim -2.5$. The rise, which is hinted at by the lower metallicity tail of our sample, is consistent with the robust rise from the Cayrel et al. (2003) sample. The regression line for $[\text{Zn}/\text{Fe}]$ provided in Table 7 of Cayrel et al. (2003) intercepts the solar ratio for $[\text{Fe}/\text{H}] \sim -2.1$. It is worth noting that our data are consistent with the data of both Mishenina et al. (2002) and Gratton et al. (2003) over the common metallicity range, and that our Zn abundances are derived from $\text{Zn I } 3302.58 \text{ \AA}$, while the other groups use optical lines. Two stars, HD 166913 and HD 132475, however, seem to defy agreement, by presenting $[\text{Zn}/\text{Fe}]$ greater than 0.45. In the case of HD 166913, the apparent high ratio $[\text{Zn}/\text{Fe}] = 0.45$ stems not from the Zn abundance itself, which is 0.11 dex above that derived by Gratton et al. (2003) (once the different atmospheric parameters are taken into account, using the abundance sensitivities given in Table 2 for HD 94028), but rather from our much lower Fe abundance, adopted from Thévenin et al. (1998) and 0.23 dex lower than Gratton et al.'s (2003). For the latter comparison, we use the abundance sensitivities from Gratton et al. (2003; Table 9), since none are given in Thévenin et al. (1998). In the case of HD 132475, the high ratio $[\text{Zn}/\text{Fe}] = 0.50$ stems from its reddening, $E(b - y) = 0.046$ (Schuster & Nissen 1989), because this reddening implies an appreciably higher effective temperature and thus a lower ratio $[\text{Zn}/\text{Fe}]$ (if referred to Table 9, Gratton et al. 2003).

⁴ In this reference, no $[\text{Cu}/\text{Fe}]$ value is given for HD 140283. We refer to the value derived from the point at the corresponding metallicity in Fig. 9.

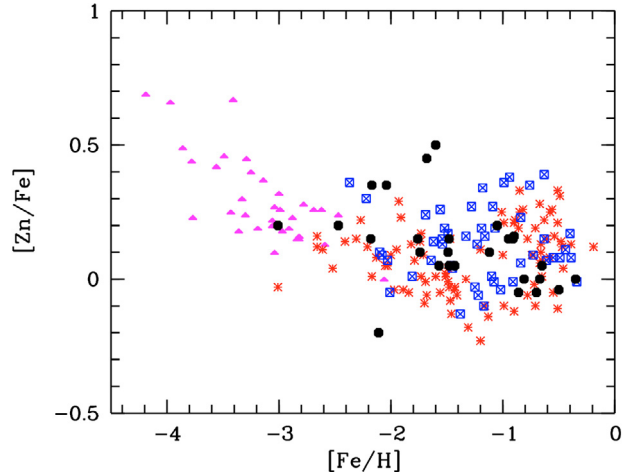


Fig. 7. $[\text{Zn}/\text{Fe}]$ ratios vs. $[\text{Fe}/\text{H}]$ from our measurements (*filled dots*), from Cayrel et al. (*filled triangles*), from Mishenina et al. (*asterisks*) and Gratton et al. (*crossed squares*). The $[\text{Zn}/\text{Fe}]$ values of Gratton et al. are decreased by 0.09 dex for normalization to meteoritic rather than to solar abundances.

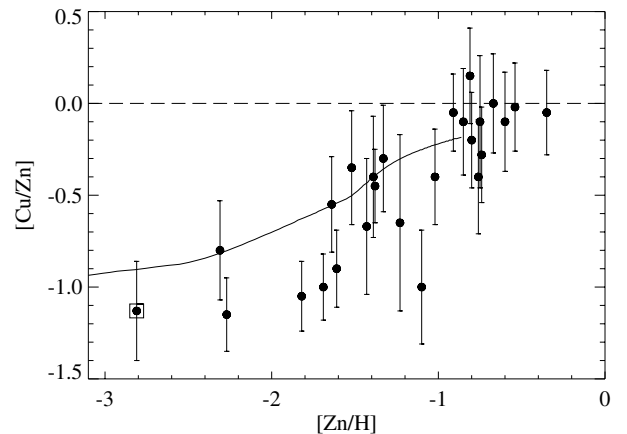


Fig. 8. $[\text{Cu}/\text{Zn}]$ ratios vs. $[\text{Zn}/\text{H}]$. The *solid line* represents the predictions of the Prantzos model.

4.2. Cu and Zn nucleosynthesis

In spite of considerable theoretical effort, the production sites of Cu and Zn are not clear (e.g. the discussion in Mishenina et al. 2002, and references therein).

- From the theoretical point of view both elements may be synthesized in massive stars. Both may be formed through n-capture during He-burning in hydrostatic equilibrium (Woosley & Weaver 1995). In addition, Cu may also be formed in explosive Ne-burning (Woosley & Weaver 1995), while Zn may be formed in explosive Si-burning and consequent α -rich freeze-out (Arnett et al. 1971). A minor contribution to both elements may come from the s-process in intermediate mass stars (Gallino et al. 1998). Also, Type Ia SNe may contribute their fraction of Cu and Zn (Iwamoto et al. 1999). Finally, there are suggestions that there might be contributions from the r-process (Woosley & Weaver 1995; Umeda & Nomoto 2002). The relative importance of all these potentially relevant processes remains to be evaluated.

- From the observational point of view some of these nucleosynthetic channels may be either ruled out or at least relegated to a very minor role.

The very different behavior of Cu and Zn implies that n-capture during He-burning cannot be the main mode of production for both. Concerning the production of Zn, there are reasons to believe that neither the *s*- nor the *r*-process can be very relevant (Cayrel et al. 2003). If the *s*-process were important, the [Zn/Fe] ratio ought to decrease with decreasing metallicity, as is the case for typical *s*-process products such as Y, Sr or Ba. From Fig. 7, it is instead clear that this ratio is initially constant and then *increases* at lower metallicities. This observational argument supports the conclusions drawn from the theoretical computations of Gallino et al. (1998). Concerning the relevance of the *r*-process, we may note that in the very metal-poor star CS 31082-001 ([Fe/H] = -2.90), in which all the *r*-process elements are greatly enhanced, [Zn/Fe] = +0.18 (Hill et al. 2002), remarkably similar to the behaviour of other stars of comparable metallicity.

We may also extend the above argument to Cu; in fact, no Cu is detected in CS 31082-001, although no upper limit is published. A greatly enhanced Cu would surely be detected in the high quality data of Hill et al. (2002). Therefore we may conclude that strong Cu production in the *r*-process is unlikely.

We compare our results with new chemical evolution predictions from Prantzos (2003, private communication), which follow those from Goswami & Prantzos (2000). The model is based on the stellar initial mass function (IMF) from Kroupa et al. (1993) and assume an evolution of the halo for a gas outflow rate which is equal to 8 times the star formation rate. We find that the Prantzos model (2003) agrees most reasonably with the observations – especially for Cu, except for some points (see Fig. 6). Model and observations agree on the existence of a plateau for Cu at very low metallicities ([Fe/H] < -2.5). This supports the adopted SNII yields (Woosley & Weaver 1995) averaged over the stellar initial mass function from Kroupa et al. (1993). Nevertheless, we stress that since higher ratios than those predicted are also observed at low metallicity (Snedden et al. 1991; Mishenina et al. 2002), we can only conclude on a possibly lower limit for the relative production of copper. As for Zn, we observe local agreements and a systematic disagreement appearing at [Fe/H] < -2, indicating, to a first approximation, that some Zn sources are missing.

5. Conclusions

In summary, we present Cu and Zn abundances for a sample of 38 stars, principally dwarfs, with metallicities ranging from solar to -3. The abundances were obtained using the intense UV lines Cu I 3273.95 Å and Zn I 3302.58 Å, and were generally in agreement with the results from previous studies. We showed that the Cu abundance indicator is adequate for the study of abundances in very metal-poor stars, permitting us to detect [Cu/Fe] ~ -1 in dwarfs at [Fe/H] = -3. This research can be extended to dwarf stars of even lower metallicities and with high resolution spectra. Contrary to the slanted s-shape trend found for [Cu/Fe], the [Zn/Fe] trend is

approximately solar in most stars with [Fe/H] > -2; this is a common result, which supports the use of Zn as a metallicity tracer in damped Ly α systems. However, at [Fe/H] < -2, Zn appears to be slightly overabundant (\langle [Zn/Fe] \rangle = +0.18) and it is in fact at these metallicities that the rise also becomes noticeable in the sample of stars studied by Cayrel et al. (2003).

The trends found can be reasonably reproduced by the halo chemical evolution predictions from Prantzos (2003, private communication). The ratio [Cu/Fe] ~ -1 for -3 < [Fe/H] < -2.5 is predicted in the Prantzos model for SNII yields from Woosley & Weaver (1995). It probably represents, at this evolutionary stage, a lower limit of Cu production, since greater ratios are also observed in previous studies. The [Zn/Fe] trend is in good general agreement with that predicted, except in the low-metallicity tail, where the predicted ratios should be systematically increased.

Acknowledgements. We would like to thank Peter A. Bergbusch and Don A. Vandenberg for providing the software producing the isochrones, and François Thévenin for information about the Catalogue III/193. We would also like to thank Robert L. Kurucz for information about the intense copper lines and their hyperfine structure, Nicolas Prantzos for providing the unpublished trends of copper and zinc, and Bertrand Plez for the TurboSpectrum code. This research has made use of the SIMBAD database, operated at CDS, Strasbourg, France, and also of data results from the Two Micron All Sky Survey, which is a joint project of the University of Massachusetts and the Infrared Processing and Analysis Center, funded by the National Aeronautics and Space Administration and the National Science Foundation.

References

- Allen, C. W. 1976, in *Astrophysical Quantities* (London: Athlone Press), 161
- Allende Prieto, C., García López, R. J., Lambert, D. L., & Gustafsson, B. 1999, *ApJ*, 527, 879
- Alonso, A., Arribas, S., & Martínez-Roger, C. 1994, *A&AS*, 107, 365
- Alonso, A., Arribas, S., & Martínez-Roger, C. 1995, *A&A*, 297, 197
- Alonso, A., Arribas, S., & Martínez-Roger, C. 1996, *A&A*, 313, 873
- Alonso, A., Arribas, S., & Martínez-Roger, C. 1998, *A&AS*, 131, 209
- Alonso, A., Arribas, S., & Martínez-Roger, C. 1999a, *A&AS*, 139, 335
- Alonso, A., Arribas, S., & Martínez-Roger, C. 1999b, *A&AS*, 140, 261
- Alvarez, R., & Plez, B. 1998, *A&A*, 330, 1109
- Anders, E., & Grevesse, N. 1989, *Geochim. Cosmochim. Acta*, 53, 197
- Arnett, W. D., Truran, J. W., & Woosley, S. E. 1971, *ApJ*, 165, 87
- Bergbusch, P. A., & Vandenberg, D. A. 2001, *ApJ*, 556, 322
- Castelli, F., Gratton, R. G., & Kurucz, R. L. 1997, *A&A*, 318, 841
- Castro, S., Porto de Mello, G. F., & Silva, L. 1999, *MNRAS*, 305, 693
- Carney, B. W., & Aaronson, M. 1979, *AJ*, 84, 867
- Cayrel de Strobel, G., Hauck, B., François, P., et al. 1992, *A&AS*, 95, 273
- Cayrel, R., et al. 2003, [[ArXiv: astro-ph/0311082](https://arxiv.org/abs/astro-ph/0311082)]
- Chen, Y. Q., Nissen, P. E., Zhao, G., Zhang, H. W., & Benoni, T. 2000, *A&AS*, 141, 491
- Cohen, J. G. 1978, *ApJ*, 223, 487
- Cohen, J. G. 1979, *ApJ*, 231, 751
- Cohen, J. G. 1980, *ApJ*, 241, 981
- Fulbright, J. P. 2000, *ApJ*, 120, 1841
- Gallino, R., Arlandini, C., Busso, M., et al. 1998, *ApJ*, 497, 388

- Goswami, A., & Prantzos, N. 2000, *A&A*, 359, 191
- Gratton, R. G., Sneden, C., Carretta, E., & Bragaglia, A. 2000, *A&A*, 354, 169
- Gratton, R. G., Carretta, E., Claudi, R., Lucatello, S., & Barbieri, M. 2003, *A&A*, 404, 187
- Hill, V., Plez, B., Cayrel, R., et al. 2002, *A&A*, 387, 560
- Israelian, G., & Rebolo, R. 2001, *ApJ*, 557, L43
- Israelian, G., Rebolo, R., García López, R. J., et al. 2001, *ApJ*, 551, 833
- Iwamoto, K., Brachwitz, F., Nomoto, K., et al. 1999, *ApJS*, 125, 439
- Kupka, F. G., Piskunov, N. E., Ryabchikova, T. A., Stempels, H. C., & Weiss, W. W. 1999, *A&AS*, 138, 119
- Kurucz, R. L. 1992, private communication
- Kurucz, R. L. 1993, CD ROM 13
- Kurucz, R. L. 1995, CD-ROM 13
- Kurucz, R. L. 2003, private communication
- Kurucz, R. L., Furenlid, I., Brault, J., & Testerman, L. 1984, Solar flux atlas from 296 to 1300 nm, National Solar Observatory
- Kroupa, P., Tout, C., & Gilmore, G. 1993, *MNRAS*, 262, 545
- Laird, J. B., Carney, B. W., & Latham, D. W. 1988, *AJ*, 95, 1843
- Luck, R. E., & Bond, H. E. 1985, *ApJ*, 292, 559
- Mishenina, T. V., & Kovtyukh, V. V. 2001, *A&A*, 370, 951
- Mishenina, T. V., Kovtyukh, V. V., Soubiran, C., Travaglio, C., & Busso, M. 2002, *A&A*, 396, 189
- Nissen, P. E., Høg, E., & Schuster, W. J. 1997, in *Hipparcos, Venice '97*, ESA SP-402 (Noordwijk: ESA), 225
- Perryman, M. A. C., et al. 1997, *The Hipparcos and Tycho Catalogues*, ESA SP-1200 (Noordwijk: ESA)
- Peterson, R. C. 1981, *ApJ*, 244, 989
- Prantzos, N. 2003, private communication
- Prochaska, J. X., Naumov, S. O., Carney, B. W., McWilliam, A., & Wolfe, A. M. 2000, *AJ*, 120, 2513
- Schuster, W. J., & Nissen, P. E. 1989, *A&A*, 222, 69
- Simmerer, J., Sneden, C., Ivans, I. I., et al. 2003, *AJ*, 125, 2018
- Sneden, C. 1973, *ApJ*, 184, 839
- Sneden, C., & Crocker, D. A. 1988, *ApJ*, 335, 406
- Sneden, C., Gratton, R. G., & Crocker, D. A. 1991, *A&A*, 246, 354
- Spite, F., & Spite, M. 1982, *A&A*, 115, 357
- Thévenin, F. 1998, *Bull. CDS* 49, Catalogue III/193
- Thévenin, F. 2003, private communication
- Thévenin, F., & Idiart, T. P. 1999, *ApJ*, 521, 753
- Umeda, H., & Nomoto, K. 2002, *ApJ*, 565, 385
- Woolsey, S. E., & Weaver, T. A. 1995, *ApJS*, 101, 181